CN bond orientation in metal carbonitride endofullerenes: A density functional theory study*

Zhu-Xia Zhang(张竹霞)[1,2,3,†], Yong Zhang(张勇)[1,2], Wen-Hua Xue(薛文华)[1,2], Wei Jia(贾伟)[1,2], Cai-Li Zhang(张彩丽)[1], Chun-Xia Li(李春霞)[4], and Peng Cui(崔鹏)[5,‡]

[1] *Key Laboratory of Interface Science and Engineering in Advanced Materials of Ministry of Education, Taiyuan University of Technology, Taiyuan* 030024, *China*

[2] *Research Center of Advanced Materials Science and Technology, Taiyuan University of Technology, Taiyuan* 030024, *China*

[3] *Collaborative Innovation Center for Shanxi Advanced Permanent Magnetic Materials and Technology, Linfen* 041004, *China*

[4] *School of Electronic Information Engineering, Yangtze Normal University, Chongqing* 408100, *China*

[5] *School of Information, Guizhou University of Finance and Economics, Guiyang* 550025, *China*

(Received 2 August 2017; revised manuscript received 25 September 2017; published online 20 November 2017)

The geometric and electronic structures of scandium carbonitride endofullerene $Sc_3CN@C_{2n}$ ($2n = 68$, 78, 80, 82, and 84) and $Sc(Y)NC@C_{76}$ have been systematically investigated to identify the preferred position of internal C and N atoms by density functional theory (DFT) calculations combined with statistical mechanics treatments. The CN bond orientation can generally be inferred from the molecule stability and electronic configuration. It is found that $Sc_3CN@C_{2n}$ molecules have the most stable structure with C atom locating at the center of Sc_3CN cluster. The CN bond has trivalent form of $[CN]^{3-}$ and connects with adjacent three Sc atoms tightly. However, in $Sc(Y)NC@C_{76}$ with $[NC]^-$, the N atom always resides in the center of the whole molecule. In addition, the stability of $Sc_3CN@C_{2n}$ has been further compared in terms of the organization of the corresponding molecular energy level. The structural differences between $Sc_3CN@C_{2n}$ and $Sc_3NC@C_{2n}$ are highlighted by their respected infrared spectra.

Keywords: geometric and electronic structures, metal carbonitride endofullerenes, theoretical calculations, CN bond orientation

PACS: 31.15.E–, 36.20.Kd, 36.40.Mr, 68.55.ap **DOI:** 10.1088/1674-1056/26/12/123102

1. Introduction

To date, numerous endohedral metallofullerenes (EMFs) with diversified encaged species and various carbon cages have been isolated owing to their complicated structures, diversified electronic properties, and potential applications in biomedicine, electronics, photovoltaics, and many other fields.[1–7] The structure and electronic properties of EMFs encaging metal atom(s), trimetallic nitride, metal carbide, metal oxide, metal sulfide, metal carbonitride, and metal cyanide have been extensively investigated.[6,8–10] For instance, the charge distribution and aromaticity of these systems are key in determining the most favorable isomeric cages for EMF encapsulation.[11,12] The chemical reactivity of some of the studied systems has also been explored.[13,14]

Considering pronounced Coulomb repulsion between two or more metal atoms, the presence of the negatively charged nonmetal atoms or clusters, e.g., carbon, nitrogen, oxygen, sulfur, carbonitride, and cyanide, is necessary to stabilize multi-metal clusters. In 1999, the first metal nitride clusterfullerene $Sc_3N@C_{80}$-I_h was reported.[15] In 2001, the metal carbide clusterfullerene $Sc_2C_2@C_{84}$ was isolated.[16] Since then, more EMFs such as $Sc_3C_2@C_{80}$-I_h,[17] $Sc_2C_2@C_{82}$-$C_{3v}(8)$,[18] $Sc_2C_2@C_{84}$-$D_{2d}(23)$,[19] and $Sc_4C_2@C_{80}$-I_h[20] were revealed. Among them, the encapsulated C_2 moiety displays complicated charge states. C_2^{2-} was found in $Sc_2C_2@C_{84}$,[19] $Sc_2C_2@C_{68}$,[21] $Ti_2C_2@C_{78}$,[22,23] and $La_2C_2@C_{90-98}$.[24] A C_2^{3-} moiety was disclosed in $Sc_3C_2@C_{80}$[17] and a C_2^{6-} anion could exist in $Sc_4C_2@C_{80}$.[20] In 2010, metal carbonitride endofullerene $Sc_3CN@C_{80}$-I_h with a CN bond was predicted by density functional theory (DFT) calculation.[25,26] Soon after that, $Sc_3CN@C_{80}$[27] and $Sc_3CN@C_{78}$[28] containing planar quinary cluster Sc_3CN were experimentally verified. The single crystal x-ray crystallographic study on $Sc_3CN@C_{80}$ failed to distinguish the position of endohedral carbon atom and nitrogen atom because of their similar electron density and size. In this context, theoretical calculations with DFT have been quite helpful. For example, Lu *et al.* explored the $Sc_3CN@C_{2n}$ ($2n = 68$, 78, and 80) and reported that all initial isomers with C atom residing at the center of the Sc_3 plane are all energetically favorable.[25] Recently, theoretical calculations have also been performed to explore the structures and electronic prop-

*Project supported by the National Natural Science Foundation of China (Grant Nos. 21503208, 61604104, and 51002102), the Natural Science Foundation of Shanxi Province, China (Grant Nos. 2015011034, 201601D202034, and 201601D202029), and the Natural Science Foundation Project of Chongqing Science and Technology Commission, China (Grant No. cstc2014jcyjA00032).

†Corresponding author. E-mail: zhangzhuxia@tyut.edu.cn

‡Corresponding author. E-mail: pcui@ustc.edu.cn

© 2017 Chinese Physical Society and IOP Publishing Ltd

erties of $Sc_3CN@C_{2n}$ ($2n = 82$ and 84) with N atom residing at the center of the Sc_3 plane.[29,30] Moreover, the monometallic carbonitride endofullerene (or metal cyanide endofullerene) of $YCN@C_s(6)$-C_{82} and $TbCN@C_s(6)$-C_{82} has been successfully synthesized and isolated, whose electronic structures were proposed as $[Y(Tb)^{3+}(CN)^-]^{2+}@[C_{82}]^{2-}$ by DFT calculation with a special triangular Y(Tb)CN cluster.[31–34] Wang *et al*. explored $MCN@C_{76}$ (M = Sc, Y) using DFT calculations and demonstrated that the entrapped MCN cluster is linear with C atom locating in the center of molecule.[35] Recently, Yang *et al.* report the syntheses and isolations of novel non-IPR (IPR: isolated pentagon rule) mononuclear clusterfullerenes $MNC@C_{76}$ (M = Tb, Y), in which one pair of strained fused-pentagon is stabilized by a nearly linear MNC mononuclear cluster.[36] $YCN@C_{78}$ has also been studied theoretically with a triangular YCN cluster.[37] Apparently, these metal carbonitride endofullerene could have variable inner CN unit with different charging states and coordinating modes. It is thus highly desirable to carry out a systematical investigation on the family of metal carbonitride endofullerenes $Sc_3CN@C_{2n}$ ($2n = 68$, 78, 80, 82, and 84) and $Sc(Y)NC@C_{76}$ to define the general relationship between the molecule structure and CN bond orientation.

2. Computational method

All isomers were derived from the reported results without considering the different cages. The endohedral C and N positions were alternated, named as $Sc_3CN@C_{2n}$ (with C atom at the center of Sc_3 plane) and $Sc_3NC@C_{2n}$ (with N atom at the center of Sc_3 plane), respectively, to understand their relative stability. For monometal cyanide endofullerene, $MCN@C_{76}$ and $MNC@C_{76}$ also represent two isomers with different CN orientations defined in a similar way as for $Sc_3CN@C_{2n}$.

The geometry optimizations were carried out with no symmetry constrain using the Gaussian 09 program. DFT methods, including PW91PW91, BP86, TPSSTPSS, M06L, B3LYP, B3PW91, PBE1PBE, BHandHLYP, CAM-B3LYP, and wb97xd, were employed for full geometry optimization. The calculated relative energies and the key structure and electronic parameters are shown in Table 1. Depending on the HF exchange contributions in these functionals, the HOMO–LUMO (highest occupied molecular orbital–lowest unoccupied molecular orbital) energy gap changes significantly. However, all DFT results indicated that $Sc_3CN@C_{2n}$ isomers are energetically stable compared to $Sc_3NC@C_{2n}$, and the calculated C–N distances in Sc_3CN cluster by each DFT method are almost same, which suggests that all DFT methods employed here show similar performance in the description of the geometry stabilities of metal carbonitride endofullerenes system. Moreover, all geometries were characterized by harmonic vibrational frequency analysis to enable to investigate enthalpy-entropy effect and infrared spectroscopy (IR) at the B3LYP level. The standard 6-31G(d) basis set for C, N, and Sc with the effective core potentials of Dolg *et al*.,[38,39] together with the optimized basis set for the valence shells with a contraction scheme of (8s7p6d2f1g)/[6s5p3d2f1g] for Y, was employed.

Table 1. All the optimized $Sc_3CN@C_{2n}$/$Sc_3NC@C_{2n}$ and $Sc(Y)NC@C_{76}$/$Sc(Y)CN@C_{76}$ isomers, their relative bonding energies (ΔE_b, in units kcal·mol^{-1}), HOMO–LUMO gaps (gap, in unit eV), encaged C–N bond length (d (C–N), in unit Å), and the dipole moment (D, in unit Debye).

	ΔE_b	Gap	d (C–N)	D
$Sc_3CN@C_{68}$/$Sc_3NC@C_{68}$	0/17.1	2.12/2.05	1.26/1.26	0.86/1.08
$Sc_3CN@C_{78}$/$Sc_3NC@C_{78}$	0/15.2	2.23/2.05	1.24/1.25	0.66/0.29
$Sc_3CN@C_{80}$/$Sc_3NC@C_{80}$	0/10.8	2.17/2.29	1.27/1.28	1.78/3.10
$Sc_3CN@C_{82}$/$Sc_3NC@C_{82}$	0/13.6	2.07/2.09	1.28/1.28	3.31/3.77
$Sc_3CN@C_{84}$/$Sc_3NC@C_{84}$	0/15.2	2.04/2.05	1.28/1.29	3.42/3.95
$ScCN@C_{76}$/$ScNC@C_{76}$	2.7/0	1.36/1.36	1.17/1.18	2.61/2.43
$YCN@C_{76}$/$YNC@C_{76}$	3.7/0	1.39/1.39	1.17/1.18	2.54/2.36

3. Results and discussion

The C_{68} (D_3: 6140),[25] C_{78} (C_2: 22010),[25,28] C_{80} (I_h: 7),[27] C_{82} (C_{2v}: 39705),[29] and C_{84} (C_s: 51365)[30] were assigned in $Sc_3CN@C_{2n}$ molecules. Among them, C_{80} (I_h: 7) has IPR-type fullerene cages, and C_{68} (D_3: 6140), C_{78} (C_2: 22010), C_{82} (C_{2v}: 39705), and C_{84} (C_s: 51365) have non-IPR-type cages. In Table 1, the calculated relative bonding energies, HOMO–LUMO gaps, and other parameters at B3LYP level are listed. The results show that $Sc_3CN@C_{2n}$ species are about 10.8 kcal·mol^{-1} ∼ 17.1 kcal·mol^{-1}, more stable than $Sc_3NC@C_{2n}$ molecules. Figure 1 presents all of the most stable isomers under investigations. The Sc_3CN

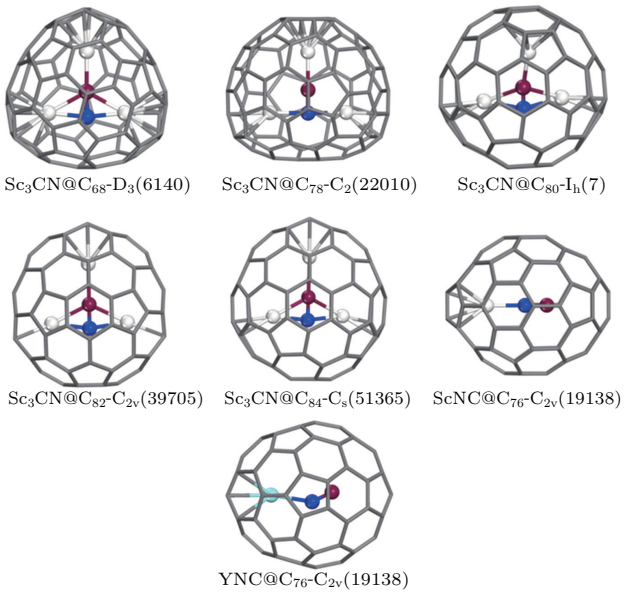


Fig. 1. (color online) The calculated $Sc_3CN@C_{2n}$ ($2n = 68$, 78, 80, 82, and 84) and $Y(Sc)NC@C_{76}$. N, Sc, and C atoms in cage are blue, white, and grey, respectively. The C atom inside cage is highlighted in purple.

clusters in $Sc_3CN@C_{2n}$ are quasi-planar with the carbon atom in the center and nitrogen atom locating on one side of the triangle formed by the Sc atoms. The HOMO–LUMO gaps and C–N bond lengths found in this study are in good agreement with previous reported data.[25,28,29,35] The change of the dipole moment is normally small when altering the CN orientation, except for that of $Sc_3CN@C_{80}$. The large variation in $Sc_3CN@C_{80}$ is due to the slight fold of Sc_3CN compared to the planar Sc_3NC.

Wang *et al.* investigated the relative energies and stabilities of $Sc(Y)CN@C_{76}$.[35] Here, we also made a comparative study on this type of molecules. Our calculations indicate that ScNC and YNC are still put in the most stable C_{76}^{2-}(C_{2v}: 19138) structure. N atom is in the center of cage in both structures. $Sc(Y)NC@C_{76}$ are more stable than $Sc(Y)CN@C_{76}$ by 2.2 and 3.3 kcal·mol^{-1}, respectively. The calculated N–C and Y–N bond lengths for $YNC@C_{76}$-C_{2v}(19138) are 1.18 Å and 2.21 Å and the M–N–C bond angle is 144.7°, which agree well with the experimental results of Yang.[36]

3.1. Temperature-dependent yield

Although $Sc_3CN@C_{2n}$ isomers are energetically stable compared to $Sc_3NC@C_{2n}$, their relative stabilities at high temperature is still not known. We have thus performed statistical thermodynamic analysis for these metal carbonitride endofullerenes. To evaluate the temperature effect, the relative concentrations of $Sc_3CN@C_{2n}$ isomers were calculated according to the formula given in Ref. [40] with the consideration of the enthalpy–entropy effect. As depicted in

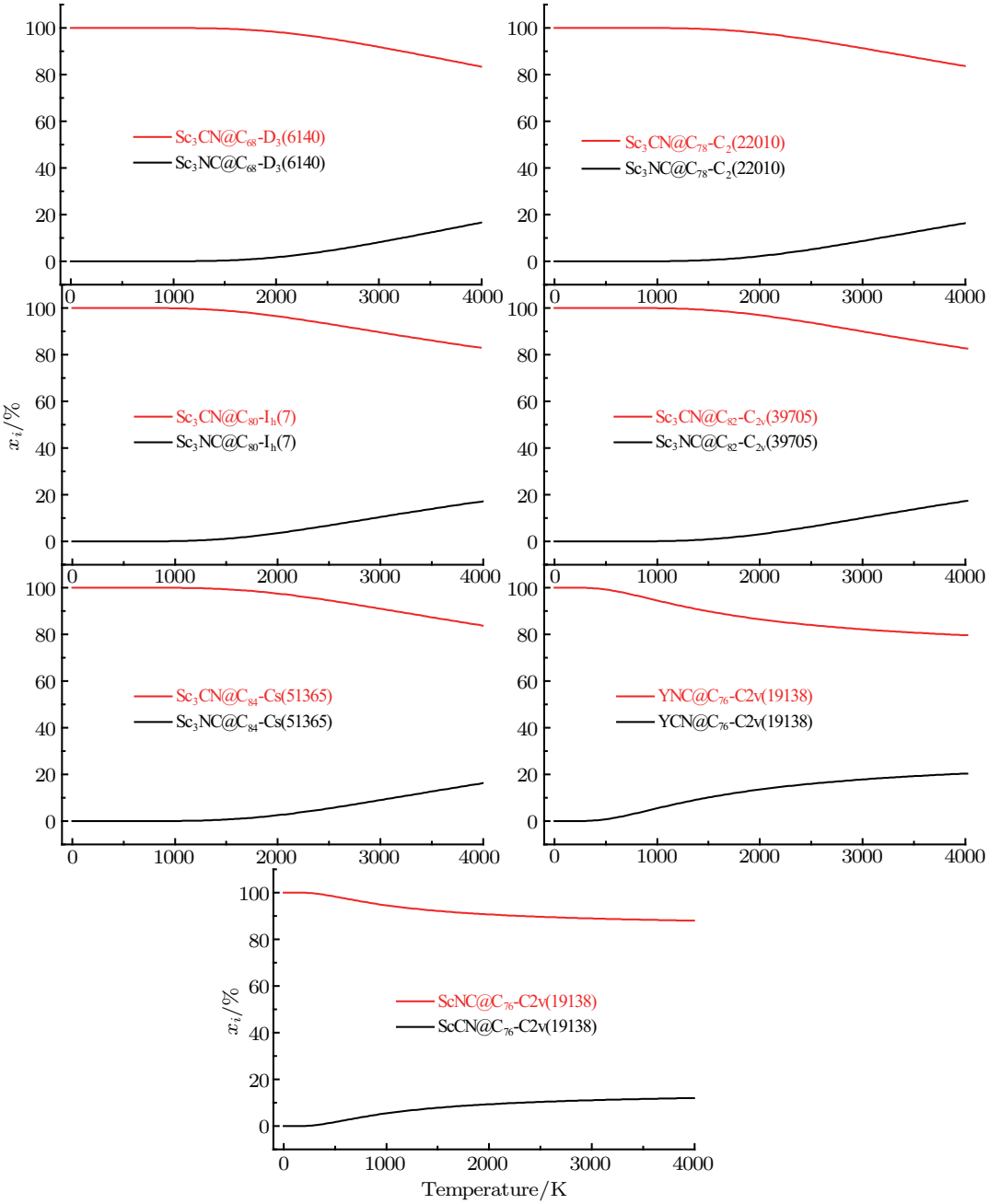


Fig. 2. (color online) Temperature-dependent molar fractions (x_i) of the carbonitride endofullerenes.

Fig. 2, the concentration of $Sc_3NC@C_{2n}$ is noticeably increased with the increase of temperature. Even so, it is obvious that all $Sc_3CN@C_{2n}$ structures exhibit superior concentration at all temperatures. It is thus reasonable to conclude that $Sc_3CN@C_{2n}$ is the major isomer in the products.

YNC@C_{76} isomer is about 3.3 kcal·mol^{-1} more stable than YCN@C_{76} at 0 K and is also highly stable in the whole temperature range (Fig. 2). The curve of the YCN@C_{76} structure slides up slowly after 500 K and reaches only 20.3% in 4000 K. The same trend can be observed for ScCN@C_{76}.

3.2. The charge state of the cyanide

It is natural that Sc_3CN is more stable (8.29 kcal·mol^{-1}) than Sc_3NC, because C is four-coordinated and N likes three-coordination. The charge state of the trapped CN unit in fullerene is an important factor for determining the Sc_3CN geometric configuration. For Sc(Y)NC@C_{76}, the valence state can be approximately described as $[Sc(Y)^{3+}(NC)^{-}]^{2+}@[C_{76}]^{2-}$. As shown in Fig. 3, the natural population of the N atom is more negative than C atom in CN^- anion. It is thus more reasonable that the N atom locates in the center of the cage and coordinates with Sc(Y) atoms directly.

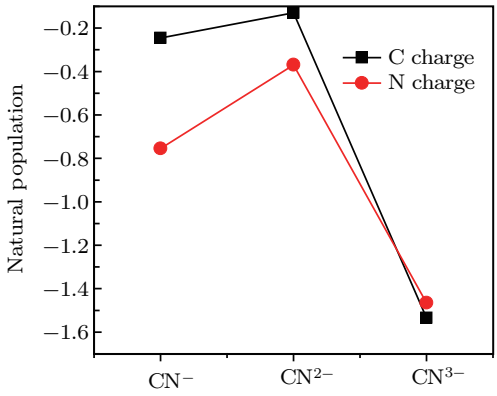


Fig. 3. (color online) Natural population of C and N atoms in CN^{n-}.

With the increasing of negative charge of CN, C atom possesses more electrons, which means that the C can tend to coordinate with metal cations. This explains why the C atoms always locate at the center of Sc_3 plane to form more bonds with Sc in $Sc_3CN@C_{2n}$ molecules whose electronic structures were described as $[Sc_3^{3+}(CN)^{3-}]^{6+}@[C_{2n}]^{6-}$.

3.3. The electronic configurations of Sc_3CN and Sc_3NC

We have also paid attention to the electronic structure of the isolated Sc_3CN and Sc_3NC clusters. It is helpful to understand the structural stability by analyzing their molecular orbitals (MOs). Figure 4 shows their frontier MOs in the ground state. In general, MOs in both clusters have very similar organization, except the relative positions of HOMO-2 and HOMO-3. Sc_3CN has the large gap between HOMO-2 and HOMO-3 and is easier to transfer six electrons to cage when it is encaged in cage, which can be an important factor to determine $Sc_3CN@C_{80}$ superior stability.

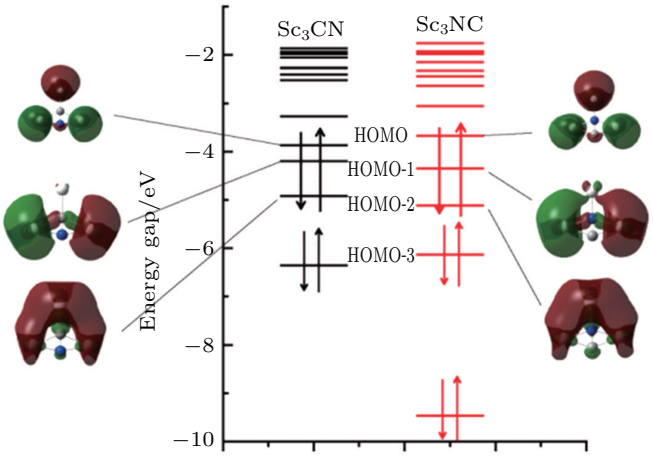


Fig. 4. (color online) The molecular energy levels of Sc_3CN and Sc_3NC.

3.4. IR spectrum

IR spectroscopy is a powerful tool for distinguishing the geometric structure of EMFs, from which the C–N bond orientation in scandium cyanide clusters can also be inferred. Here we focus on analyzing the vibrations of CN unit in above mentioned two isomers. In Fig. 5, the simulated IR spectra of $Sc_3CN@C_{2n}$ and $Sc_3NC@C_{2n}$ are presented for comparison.

For most EMFs, their IR spectra can be roughly classified into three bands: from 1000 cm^{-1} to 1700 cm^{-1}, from 300 to 900 cm^{-1}, and blow 200 cm^{-1}. The first two bands are contributed by the vibrations of the carbon cages. The third band mainly comes from the inner clusters. Notably, the IR spectral features of $Sc_3CN@C_{68}$ in the high-energy range (related to the internal cluster) are similar to those of $Sc_3NC@C_{68}$, because large strain between embedded cluster Sc_3CN (Sc_3NC) and cage masks the differences from different positions of C and N atoms. However, for those with larger fullerene cages, the IR spectral features in the high-energy range show slight differences between $Sc_3CN@C_{2n}$ and $Sc_3NC@C_{2n}$. For example, the IR vibrations in high-energy range for $Sc_3CN@C_{78}$ are different from those in $Sc_3NC@C_{78}$. In detail, the signals (405 and 265 cm^{-1} for $Sc_3CN@C_{78}$ and $Sc_3NC@C_{78}$, respectively) are assigned to the C (or N)-dominated (Sc–C–Sc or Sc–N–Sc) stretch modes.

The C–N stretching frequencies (marked with black star) of the central CN units (1767, 1809, 1689, 1618, and 1588 cm^{-1} for $Sc_3CN@C_{68}$, $Sc_3CN@C_{78}$, $Sc_3CN@C_{80}$, $Sc_3CN@C_{82}$, and $Sc_3CN@C_{84}$, respectively) have very weak absorption intensities. The corresponding stretching modes (marked with red star) from $Sc_3NC@C_{68}$ to $Sc_3NC@C_{84}$

for $Sc_3NC@C_{2n}$ species change to 1653, 1699, 1534, 1515, and 1504 cm^{-1}, respectively. Their absorption intensities are slighter stronger than those in $Sc_3CN@C_{2n}$. That is more obvious in $Sc(Y)NC@C_{76}$. There are characteristic peaks for C–N stretching frequencies at 2142 and 2141 cm^{-1} in $ScNC@C_{76}$ and $YNC@C_{76}$, respectively.

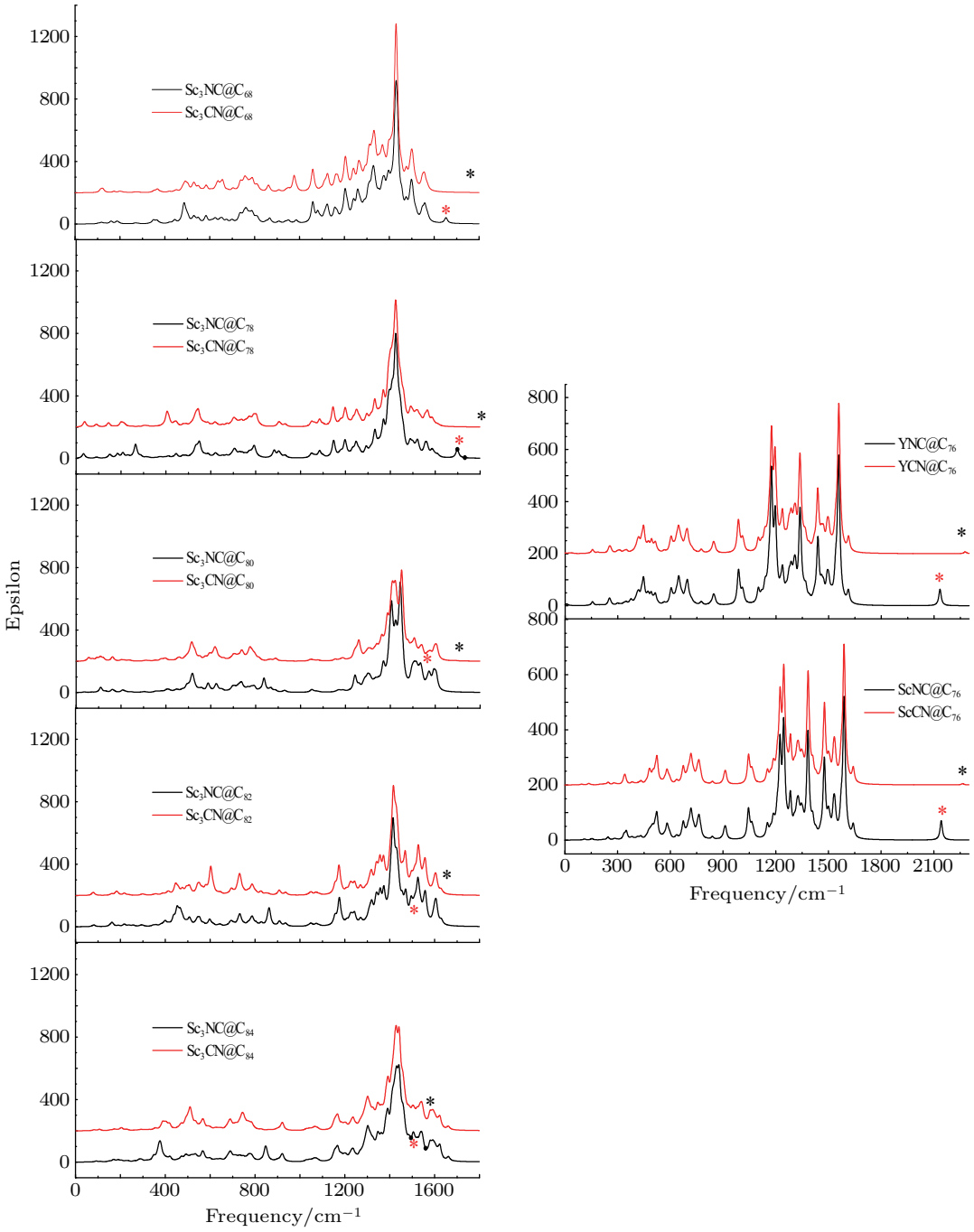


Fig. 5. (color online) The calculated IR vibration spectra. The C–N stretching frequencies were marked with star.

4. Conclusion

The positions of C and N atom in metal carbonitride endofullerenes were investigated. In $Sc_3CN@C_{2n}$ ($2n = 68$, 78, 80, 82, and 84), CN was found to have the 3-valence state, resulting in more electrons located at C atom and placing C atom at the center of Sc_3 plane. In $Sc(Y)NC@C_{76}$, the N atom becomes more negative to favor its direct bonding with metal atoms. The enthalpy–entropy effect was also considered to examine the relatively high stabilities of $Sc_3CN@C_{2n}$ and $Sc(Y)NC@C_{76}$ at elevated temperatures. It is expected that the present results will enrich the research area of the stability of metallofullerenes with complex composition and geometry.

Acknowledgment

We thank the support from the Key Laboratory of Magnetic Molecules & Magnetic Information Materials of Min-

istry of Education, Shanxi Normal University.

References

[1] Cerón M R, Li F F and Echegoyen L A 2014 *J. Phys. Org. Chem.* **27** 258

[2] Yang S, Liu F, Chen C, Jiao M and Wei T 2011 *Chem. Commun.* **47** 11822

[3] Wang T and Wang C 2014 *Acc. Chem. Res.* **47** 450

[4] Lu X, Feng L, Akasaka T and Nagase S 2012 *Chem. Soc. Rev.* **41** 7723

[5] Jin P, Tang C and Chen Z 2014 *Coord. Chem. Rev.* **270–271** 89

[6] Popov A A, Yang S and Dunsch L 2013 *Chem. Rev.* **113** 5989

[7] Tang C M, Guo W, Zhu W H, Liu M Y, Zhang A M, Gong J F and Hui W 2012 *Acta Phys. Sin.* **61** 26101 (in Chinese)

[8] Deng Q and Popov A A 2014 *J. Am. Chem. Soc.* **136** 4257

[9] Zhao R, Guo Y, Zhao P, Ehara M, Nagase S and Zhao X 2016 *J. Phys. Chem. C* **120** 1275

[10] Yang S, Wei T and Jin F 2017 *Chem. Soc. Rev.* **46** 5005

[11] Rodríguez-Fortea A, Alegret N, Balch A L and Poblet J M 2010 *Nat. Chem.* **2** 955

[12] Garcia-Borras M, Osuna S, Luis J M, Swart M and Sola M 2014 *Chem. Soc. Rev.* **43** 5089

[13] Garcia-Borràs M, Osuna S, Luis J M, Swart M and Solà M 2013 *Chem. Eur. J.* **19** 14931

[14] Osuna S, Swart M and Sola M 2011 *Phys. Chem. Chem. Phys.* **13** 3585

[15] Stevenson S, Rice G, Glass T, Harich K, Cromer F, Jordan M R, Craft J, Hadju E, Bible R, Olmstead M M, Maitra K, Fisher A J, Balch A L and Dorn H C 1999 *Nature* **401** 55

[16] Wang C R, Kai T, Tomiyama T, Yoshida T, Kobayashi Y, Nishibori E, Takata M, Sakata M and Shinohara H 2001 *Angew. Chem. Int. Ed.* **40** 397

[17] Iiduka Y, Wakahara T, Nakahodo T, Tsuchiya T, Sakuraba A, Maeda Y, Akasaka T, Yoza K, Horn E, Kato T, Liu M T H, Mizorogi N, Kobayashi K and Nagase S 2005 *J. Am. Chem. Soc.* **127** 12500

[18] Iiduka Y, Wakahara T, Nakajima K, Nakahodo T, Tsuchiya T, Maeda Y, Akasaka T, Yoza K, Liu M T H, Mizorogi N and Nagase S 2007 *Angew. Chem. Int. Ed.* **119** 5658

[19] Kurihara H, Lu X, Iiduka Y, Nikawa H, Hachiya M, Mizorogi N, Slanina Z, Tsuchiya T, Nagase S and Akasaka T 2012 *Inorg. Chem.* **51** 746

[20] Wang T S, Chen N, Xiang J F, Li B, Wu J Y, Xu W, Jiang L, Tan K, Shu C Y, Lu X and Wang C R 2009 *J. Am. Chem. Soc.* **131** 16646

[21] Shi Z Q, Wu X, Wang C R, Lu X and Shinohara H 2006 *Angew. Chem. Int. Ed.* **45** 2107

[22] Tan K and Lu X 2005 *Chem. Commun.* **0** 4444

[23] Yumura T, Sato Y, Suenaga K and Iijima S 2005 *J. Phys. Chem. B* **109** 20251

[24] Zhao S, Zhao P, Cai W, Bao L, Chen M, Xie Y, Zhao X and Lu X 2017 *J. Am. Chem. Soc.* **139** 4724

[25] Jin P, Zhou Z, Hao C, Gao Z, Tan K, Lu X and Chen Z 2010 *Phys. Chem. Chem. Phys.* **12** 12442

[26] Wang T, Wu J and Feng Y 2014 *Dalton T.* **43** 16270

[27] Wang T S, Feng L, Wu J Y, Xu W, Xiang J F, Tan K, Ma Y H, Zheng J P, Jiang L, Lu X, Shu C Y and Wang C R 2010 *J. Am. Chem. Soc.* **132** 16362

[28] Wu J, Wang T, Ma Y, Jiang L, Shu C and Wang C 2011 *J. Phys. Chem. C* **115** 23755

[29] Meng Q Y, Sun X Y, Wang C Y and Wang D L 2014 *Chem. Phys. Lett.* **613** 24

[30] Wang D L, Xu H L, Su Z M and Xin G 2012 *Phys. Chem. Chem. Phys.* **14** 15099

[31] Liu F, Wang S, Guan J, Wei T, Zeng M and Yang S 2014 *Inorg. Chem.* **53** 5201

[32] Yang S, Chen C, Liu F, Xie Y, Li F, Jiao M, Suzuki M, Wei T, Wang S, Chen Z, Lu X and Akasaka T 2013 *Sci. Rep.* **3** 1487

[33] Zheng H, Zhao X, He L, Wang W W and Nagase S 2014 *Inorg. Chem.* **53** 12911

[34] Liu F, Gao C L, Deng Q, Zhu X, Kostanyan A, Westerstrom R, Wang S, Tan Y Z, Tao J, Xie S Y, Popov A A, Greber T and Yang S 2016 *J. Am. Chem. Soc.* **138** 14764

[35] Meng Q Y, Wang D L, Xin G, Li T C and Hou D Y 2014 *Comput. Theor. Chem.* **1050** 83

[36] Liu F, Wang S, Gao C L, Deng Q, Zhu X, Kostanyan A, Westerstrom R, Jin F, Xie S Y, Popov A A, Greber T and Yang S 2017 *Angew. Chem. Int. Ed. Engl.* **56** 1830

[37] Zhao L J and Wang D L 2015 *Int. J. Quantum Chem.* **115** 779

[38] Andrae D, Häußermann U, Dolg M, Stoll H, and Preuß H 1990 *Theor. Chim. Acta* **77** 123

[39] Martin J M L and Sundermann A 2001 *J. Chem. Phys.* **114** 3408

[40] Slanina Z, Lee S L, Uhlík F, Adamowicz L and Nagase S 2006 *Theor. Chem. Acc.* **117** 315